Saturation of Azimuthal Anisotropy in Au + Au Collisions at $\sqrt{s_{NN}} = 62$–200 GeV

S. S. Adler,[5] S. Afanasiev,[20] C. Aidala,[5,10] N. N. Ajitanand,[48] Y. Akiba,[23,42,43] A. Al-Jamel,[37] J. Alexander,[48] R. Amirikas,[14] K. Aoki,[27,42] L. Aphecetche,[50] R. Armendariz,[37] S. H. Aronson,[5] R. Averbeck,[49] T. C. Awes,[38] B. Azmoun,[5] R. Azmoun,[49] V. Babintsev,[17] A. Baldisseri,[11] K. N. Barish,[6] P. D. Barnes,[30] B. Bassalleck,[36] S. Bathe,[6,33] S. Batsouli,[10] V. Baublis,[41] F. Bauer,[6] A. Bazilevsky,[5,17,43] S. Belikov,[5,17,19] R. Bennett,[49] Y. Berdnikov,[45] S. Bhagavatula,[19] M. T. Bjorndal,[10] J. G. Boissevain,[30] H. Borel,[11] S. Borenstein,[28] K. Boyle,[49] M. L. Brooks,[30] D. S. Brown,[37] N. Bruner,[36] D. Bucher,[33] H. Buesching,[5,33] V. Bumazhnov,[17] G. Bunce,[5,43] J. M. Burward-Hoy,[29,30,49] S. Butsyk,[49] X. Camard,[50] S. Campbell,[49] J.-S. Chai,[21] P. Chand,[4] W. C. Chang,[2] S. Chernichenko,[17] C. Y. Chi,[10] J. Chiba,[23] M. Chiu,[10] I. J. Choi,[57] J. Choi,[22] R. K. Choudhury,[4] T. Chujo,[5,54] V. Cianciolo,[38] C. R. Cleven,[15] Y. Cobigo,[11] B. A. Cole,[10] M. P. Comets,[39] P. Constantin,[19] M. Csanád,[13] T. Csörgő,[24] D. d'Enterria,[10,50] T. Dahms,[49] K. Das,[14] G. David,[5] H. Delagrange,[50] A. Denisov,[17] A. Deshpande,[43,49] E. J. Desmond,[5] A. Devismes,[49] O. Dietzsch,[46] A. Dion,[49] J. L. Drachenberg,[1] O. Drapier,[28] A. Drees,[49] K. A. Drees,[5] A. K. Dubey,[56] R. du Rietz,[32] A. Durum,[17] D. Dutta,[4] V. Dzhordzhadze,[51] Y. V. Efremenko,[38] J. Egdemir,[49] K. El Chenawi,[54] A. Enokizono,[16] H. En'yo,[42,43] B. Espagnon,[39] S. Esumi,[53] L. Ewell,[5] D. E. Fields,[36,43] F. Fleuret,[28] S. L. Fokin,[26] B. Forestier,[31] B. D. Fox,[43] Z. Fraenkel,[56] J. E. Frantz,[10] A. Franz,[5] A. D. Frawley,[14] Y. Fukao,[27,42] S.-Y. Fung,[6] S. Gadrat,[31] S. Garpman,[32,*] F. Gastineau,[50] M. Germain,[50] T. K. Ghosh,[54] A. Glenn,[51] G. Gogiberidze,[51] M. Gonin,[28] J. Gosset,[11] Y. Goto,[42,43] R. Granier de Cassagnac,[28] N. Grau,[19] S. V. Greene,[54] M. Grosse Perdekamp,[18,43] T. Gunji,[8] W. Guryn,[5] H.-Å. Gustafsson,[32] T. Hachiya,[16,42] A. Hadj Henni,[50] J. S. Haggerty,[5] M. N. Hagiwara,[1] H. Hamagaki,[8] A. G. Hansen,[30] H. Harada,[16] E. P. Hartouni,[29] K. Haruna,[16] M. Harvey,[5] E. Haslum,[32] K. Hasuko,[42] R. Hayano,[8] N. Hayashi,[42] X. He,[15] M. Heffner,[29] T. K. Hemmick,[49] J. M. Heuser,[42,49] M. Hibino,[55] H. Hiejima,[18] J. C. Hill,[19] R. Hobbs,[36] M. Holmes,[54] W. Holzmann,[48] K. Homma,[16] B. Hong,[25] A. Hoover,[37] T. Horaguchi,[42,52] H. M. Hur,[21] T. Ichihara,[42,43] V. V. Ikonnikov,[26] K. Imai,[27,42] M. Inaba,[53] D. Isenhower,[1] L. Isenhower,[1] M. Ishihara,[42] T. Isobe,[8] M. Issah,[48] A. Isupov,[20] B. V. Jacak,[49] W. Y. Jang,[25] Y. Jeong,[22] J. Jia,[10,49] J. Jin,[10] O. Jinnouchi,[42,43] B. M. Johnson,[5] S. C. Johnson,[29] K. S. Joo,[34] D. Jouan,[39] F. Kajihara,[8,42] S. Kametani,[8,55] N. Kamihara,[42,52] M. Kaneta,[43] J. H. Kang,[57] S. S. Kapoor,[4] K. Katou,[55] T. Kawagishi,[53] A. V. Kazantsev,[26] S. Kelly,[9,10] B. Khachaturov,[56] A. Khanzadeev,[41] J. Kikuchi,[55] D. H. Kim,[34] D. J. Kim,[57] D. W. Kim,[22] E. Kim,[47] G.-B. Kim,[28] H. J. Kim,[57] Y.-S. Kim,[21] E. Kinney,[9] W. W. Kinnison,[30] A. Kiss,[13] E. Kistenev,[5] A. Kiyomichi,[42,53] K. Kiyoyama,[35] C. Klein-Boesing,[33] H. Kobayashi,[42,43] L. Kochenda,[41] V. Kochetkov,[17] D. Koehler,[36] T. Kohama,[16] B. Komkov,[41] M. Konno,[53] M. Kopytine,[49] D. Kotchetkov,[6] A. Kozlov,[56] P. J. Kroon,[5] C. H. Kuberg,[1,30] G. J. Kunde,[30] N. Kurihara,[8] K. Kurita,[42,43,44] Y. Kuroki,[53] M. J. Kweon,[25] Y. Kwon,[57] G. S. Kyle,[37] R. Lacey,[48] V. Ladygin,[20] J. G. Lajoie,[19] Y. Le Bornec,[39] A. Lebedev,[19,26] S. Leckey,[49] D. M. Lee,[30] M. K. Lee,[57] S. Lee,[22] M. J. Leitch,[30] M. A. L. Leite,[46] X. H. Li,[6] H. Lim,[47] A. Litvinenko,[20] M. X. Liu,[30] Y. Liu,[39] C. F. Maguire,[54] Y. I. Makdisi,[5] A. Malakhov,[20] M. D. Malik,[36] V. I. Manko,[26] Y. Mao,[7,42] G. Martinez,[50] M. D. Marx,[49] H. Masui,[53] F. Matathias,[49] T. Matsumoto,[8,55] M. C. McCain,[18] P. L. McGaughey,[30] E. Melnikov,[17] F. Messer,[49] Y. Miake,[53] J. Milan,[48] T. E. Miller,[54] A. Milov,[49,56] S. Mioduszewski,[5] R. E. Mischke,[30] G. C. Mishra,[15] J. T. Mitchell,[5] A. K. Mohanty,[4] D. P. Morrison,[5] J. M. Moss,[30] T. V. Moukhanova,[26] F. Mühlbacher,[49] D. Mukhopadhyay,[54,56] M. Muniruzzaman,[6] J. Murata,[42,43,44] S. Nagamiya,[23] Y. Nagata,[53] J. L. Nagle,[9,10] M. Naglis,[56] T. Nakamura,[16] B. K. Nandi,[6] M. Nara,[53] J. Newby,[29,51] M. Nguyen,[49] P. Nilsson,[32] B. Norman,[30] A. S. Nyanin,[26] J. Nystrand,[32] E. O'Brien,[5] C. A. Ogilvie,[19] H. Ohnishi,[5,42] I. D. Ojha,[3,54] H. Okada,[27,42] K. Okada,[42,43] O. O. Omiwade,[1] M. Ono,[53] V. Onuchin,[17] A. Oskarsson,[32] I. Otterlund,[32] K. Oyama,[8] K. Ozawa,[8] D. Pal,[54,56] A. P. T. Palounek,[30] V. Pantuev,[49] V. Papavassiliou,[37] J. Park,[47] W. J. Park,[25] A. Parmar,[36] S. F. Pate,[37] H. Pei,[19] T. Peitzmann,[33] J.-C. Peng,[18,30] H. Pereira,[11] V. Peresedov,[20] D. Yu. Peressounko,[26] C. Pinkenburg,[5] R. P. Pisani,[5] F. Plasil,[38] M. L. Purschke,[5] A. K. Purwar,[49] H. Qu,[15] J. Rak,[19] I. Ravinovich,[56] K. F. Read,[38,51] M. Reuter,[49] K. Reygers,[33] V. Riabov,[41,45] Y. Riabov,[41] G. Roche,[31] A. Romana,[28] M. Rosati,[19] S. S. E. Rosendahl,[32] P. Rosnet,[31] P. Rukoyatkin,[20] V. L. Rykov,[42] S. S. Ryu,[57] M. E. Sadler,[1] B. Sahlmueller,[33] N. Saito,[27,42,43] T. Sakaguchi,[8,55] M. Sakai,[35] S. Sakai,[53] V. Samsonov,[41] L. Sanfratello,[36] R. Santo,[33] H. D. Sato,[27,42] S. Sato,[5,23,53] S. Sawada,[23] Y. Schutz,[50] V. Semenov,[17] R. Seto,[6] D. Sharma,[56] M. R. Shaw,[1,30] T. K. Shea,[5] I. Shein,[17] T.-A. Shibata,[42,52] K. Shigaki,[16,23] T. Shiina,[30] M. Shimomura,[53] T. Shohjoh,[53] K. Shoji,[27,42] A. Sickles,[49] C. L. Silva,[46] D. Silvermyr,[30,32,38] K. S. Sim,[25] J. Simon-Gillo,[30] C. P. Singh,[3] V. Singh,[3] M. Sivertz,[5] S. Skutnik,[19] W. C. Smith,[1] A. Soldatov,[17] R. A. Soltz,[29] W. E. Sondheim,[30] S. P. Sorensen,[51] I. V. Sourikova,[5] F. Staley,[11] P. W. Stankus,[38] E. Stenlund,[32] M. Stepanov,[37] A. Ster,[24] S. P. Stoll,[5] T. Sugitate,[16] C. Suire,[39] J. P. Sullivan,[30] J. Sziklai,[24] T. Tabaru,[43] S. Takagi,[53] E. M. Takagui,[46]

A. Taketani,[42,43] M. Tamai,[55] K. H. Tanaka,[23] Y. Tanaka,[35] K. Tanida,[42,43] M. J. Tannenbaum,[5] A. Taranenko,[48] P. Tarján,[12] J. D. Tepe,[1,30] T. L. Thomas,[36] M. Togawa,[27,42] J. Tojo,[27,42] H. Torii,[27,42] R. S. Towell,[1] V.-N. Tram,[28] I. Tserruya,[56] Y. Tsuchimoto,[16,42] H. Tsuruoka,[53] S. K. Tuli,[3] H. Tydesjö,[32] N. Tyurin,[17] H. Valle,[54] H. W. van Hecke,[30] J. Velkovska,[5,49,54] M. Velkovsky,[49] R. Vertesi,[12] V. Veszprémi,[12] L. Villatte,[51] A. A. Vinogradov,[26] M. A. Volkov,[26] E. Vznuzdaev,[41] M. Wagner,[27] X. R. Wang,[15,37] Y. Watanabe,[42,43] J. Wessels,[33] S. N. White,[5] N. Willis,[39] D. Winter,[10] F. K. Wohn,[19] C. L. Woody,[5] M. Wysocki,[9] W. Xie,[6,43] Y. Yang,[7] A. Yanovich,[17] S. Yokkaichi,[42,43] G. R. Young,[38] I. Younus,[36] I. E. Yushmanov,[26] W. A. Zajc,[10,†] O. Zaudkte,[33] C. Zhang,[10] S. Zhou,[7] S. J. Zhou,[56] J. Zimányi,[24] and L. Zolin[20]

(PHENIX Collaboration)

[1]*Abilene Christian University, Abilene, Texas 79699, USA*
[2]*Institute of Physics, Academia Sinica, Taipei 11529, Taiwan*
[3]*Department of Physics, Banaras Hindu University, Varanasi 221005, India*
[4]*Bhabha Atomic Research Centre, Bombay 400 085, India*
[5]*Brookhaven National Laboratory, Upton, New York 11973-5000, USA*
[6]*University of California - Riverside, Riverside, California 92521, USA*
[7]*China Institute of Atomic Energy (CIAE), Beijing, People's Republic of China*
[8]*Center for Nuclear Study, Graduate School of Science, University of Tokyo, 7-3-1 Hongo, Bunkyo, Tokyo 113-0033, Japan*
[9]*University of Colorado, Boulder, Colorado 80309, USA*
[10]*Columbia University, New York, New York 10027, USA*
and Nevis Laboratories, Irvington, New York 10533, USA
[11]*Dapnia, CEA Saclay, F-91191, Gif-sur-Yvette, France*
[12]*Debrecen University, H-4010 Debrecen, Egyetem tér 1, Hungary*
[13]*ELTE, Eötvös Loránd University, H - 1117 Budapest, Pázmány P. s. 1/A, Hungary*
[14]*Florida State University, Tallahassee, Florida 32306, USA*
[15]*Georgia State University, Atlanta, Georgia 30303, USA*
[16]*Hiroshima University, Kagamiyama, Higashi-Hiroshima 739-8526, Japan*
[17]*Institute for High Energy Physics (IHEP), Protvino, Russia*
[18]*University of Illinois at Urbana-Champaign, Urbana, Illinois 61801, USA*
[19]*Iowa State University, Ames, Iowa 50011, USA*
[20]*Joint Institute for Nuclear Research, 141980 Dubna, Moscow Region, Russia*
[21]*KAERI, Cyclotron Application Laboratory, Seoul, South Korea*
[22]*Kangnung National University, Kangnung 210-702, Korea*
[23]*KEK, High Energy Accelerator Research Organization, Tsukuba-shi, Ibaraki-ken 305-0801, Japan*
[24]*KFKI Research Institute for Particle and Nuclear Physics (RMKI), H-1525 Budapest 114, P.O. Box 49, Hungary*
[25]*Korea University, Seoul, 136-701, Korea*
[26]*Russian Research Center "Kurchatov Institute", Moscow, Russia*
[27]*Kyoto University, Kyoto 606-8502, Japan*
[28]*Laboratoire Leprince-Ringuet, Ecole Polytechnique, CNRS-IN2P3, Route de Saclay, F-91128, Palaiseau, France*
[29]*Lawrence Livermore National Laboratory, Livermore, California 94550, USA*
[30]*Los Alamos National Laboratory, Los Alamos, New Mexico 87545, USA*
[31]*LPC, Université Blaise Pascal, CNRS-IN2P3, Clermont-Fd, 63177 Aubiere Cedex, France*
[32]*Department of Physics, Lund University, Box 118, SE-221 00 Lund, Sweden*
[33]*Institut für Kernphysik, University of Muenster, D-48149 Muenster, Germany*
[34]*Myongji University, Yongin, Kyonggido 449-728, Korea*
[35]*Nagasaki Institute of Applied Science, Nagasaki-shi, Nagasaki 851-0193, Japan*
[36]*University of New Mexico, Albuquerque, New Mexico 87131, USA*
[37]*New Mexico State University, Las Cruces, New Mexico 88003, USA*
[38]*Oak Ridge National Laboratory, Oak Ridge, Tennessee 37831, USA*
[39]*IPN-Orsay, Universite Paris Sud, CNRS-IN2P3, BP1, F-91406, Orsay, France*
[40]*Peking University, Beijing, People's Republic of China*
[41]*PNPI, Petersburg Nuclear Physics Institute, Gatchina, Russia*
[42]*RIKEN (The Institute of Physical and Chemical Research), Wako, Saitama 351-0198, Japan*
[43]*RIKEN BNL Research Center, Brookhaven National Laboratory, Upton, New York 11973-5000, USA*
[44]*Physics Department, Rikkyo University, 3-34-1 Nishi-Ikebukuro, Toshima, Tokyo 171-8501, Japan*
[45]*St. Petersburg State Technical University, St. Petersburg, Russia*
[46]*Instituto de Física, Universidade de São Paulo, Caixa Postal 66318, São Paulo CEP05315-970, Brazil*
[47]*System Electronics Laboratory, Seoul National University, Seoul, Korea*

[48]Chemistry Department, Stony Brook University, Stony Brook, SUNY, New York 11794-3400, USA
[49]Department of Physics and Astronomy, Stony Brook University, SUNY, Stony Brook, New York 11794, USA
[50]SUBATECH (Ecole des Mines de Nantes, CNRS-IN2P3, Université de Nantes) BP 20722 - 44307, Nantes, France
[51]University of Tennessee, Knoxville, Tennessee 37996, USA
[52]Department of Physics, Tokyo Institute of Technology, Tokyo, 152-8551, Japan
[53]Institute of Physics, University of Tsukuba, Tsukuba, Ibaraki 305, Japan
[54]Vanderbilt University, Nashville, Tennessee 37235, USA
[55]Waseda University, Advanced Research Institute for Science and Engineering, 17 Kikui-cho, Shinjuku-ku, Tokyo 162-0044, Japan
[56]Weizmann Institute, Rehovot 76100, Israel
[57]Yonsei University, IPAP, Seoul 120-749, Korea
(Received 19 November 2004; published 17 June 2005)

New measurements are presented for charged hadron azimuthal correlations at midrapidity in Au + Au collisions at $\sqrt{s_{NN}} = 62.4$ and 200 GeV. They are compared to earlier measurements obtained at $\sqrt{s_{NN}} =$ 130 GeV and in Pb + Pb collisions at $\sqrt{s_{NN}} = 17.2$ GeV. Sizeable anisotropies are observed with centrality and transverse momentum (p_T) dependence characteristic of elliptic flow (v_2). For a broad range of centralities, the observed magnitudes and trends of the differential anisotropy, $v_2(p_T)$, change very little over the collision energy range $\sqrt{s_{NN}} = 62$–200 GeV, indicating saturation of the excitation function for v_2 at these energies. Such a saturation may be indicative of the dominance of a very soft equation of state for $\sqrt{s_{NN}} \sim 60$–200 GeV.

DOI: 10.1103/PhysRevLett.94.232302 PACS numbers: 25.75.Ld

Extremely high energy-density nuclear matter is produced in energetic Au + Au collisions at the relativistic heavy ion collider (RHIC) [1,2]. The dynamical evolution of this matter is predicted to reflect the presence and evolution of the quark gluon plasma (QGP)—a new phase of nuclear matter [3–5]. Azimuthal correlation measurements are important in several ways. They serve as a ''barometric sensor'' for pressure gradients developed in the collision and hence yield insight into crucial issues of thermalization and the equation of state (EOS) [6–8]. They provide important constraints for the density of the medium and the effective energy loss of partons which traverse it [9]. They can provide valuable information on the gluon saturation scale in the nucleus [10].

Recent measurements at RHIC ($\sqrt{s_{NN}} = 130$ and 200 GeV) indicate a mixture of (di-)jet and harmonic contributions to azimuthal correlations in Au + Au collisions [11–14]. The asymmetric (di-)jet contributions are found to be relatively small but can be separated; they show an increase with p_T and indicate strong suppression of away-side jet yields [13]. Significant modifications to the away-side jet topology have also been reported [15]. These observations, which are particularly striking for very central collisions, have been interpreted as evidence for parton energy loss and jet quenching in the produced medium [3]. The harmonic contributions show significant strength at midrapidity with characteristic dependencies on p_T and centrality [11,16–18]. They are typically characterized by the second order Fourier coefficient, $v_2 = \langle e^{i2(\phi_1 - \Phi_{\mathrm{RP}})} \rangle$, where ϕ_1 represents the azimuthal emission angle of a charged hadron and ϕ_{RP} is the azimuth of the reaction plane. The brackets denote statistical averaging over particles and events. At low p_T ($p_T \lesssim 2.0$ GeV/c) the magnitude and trends of v_2 are under-predicted by hadronic cascade models supplemented with string dynamics [19], but are well reproduced by models which incorporate hydrodynamic flow [5,7]. This has been interpreted as evidence for the production of a thermalized state of partonic matter [3–5]. At higher p_T the predictions of quark coalescence [20] are consistent with the data [18,21], and quantitative agreement has been achieved with transport model calculations which incorporate large opacities [22].

At Super Proton Synchrotron (SPS) energies ($\sqrt{s_{NN}} \sim$ 17 GeV) azimuthal correlation measurements also indicate a mixture of (di-)jet and harmonic contributions [23,24]. However, the observed anisotropy of the harmonic contribution is approximately 50% of the value observed at full RHIC energy ($\sqrt{s_{NN}} = 200$ GeV). Therefore, an important outstanding issue is the detailed behavior of v_2 over the range which spans SPS-RHIC energies. In recent work, the PHOBOS Collaboration has investigated the patterns for p_T-integrated v_2 over a broad range of pseudorapidities [25]. We present more revealing differential measurements for Au + Au collisions at $\sqrt{s_{NN}} = 62.4$–200 GeV and the first excitation function for differential v_2 which spans beam energies from the Alternating Gradient Synchrotron (AGS) to RHIC ($\sqrt{s_{NN}} \sim$ 3–200 GeV).

The colliding Au beams ($\sqrt{s_{NN}} = 62.4$, 130, and 200 GeV) used in the measurements presented here have been provided by RHIC in three separate experimental running periods (years 2004, 2000, and 2001, respectively). Charged tracks were detected in the two central arms ($|\eta| \leq 0.35$) of PHENIX [26]. Track reconstruction was accomplished at each collision energy via pattern recognition using a drift chamber (DC) followed by two layers of multiwire proportional chambers with pad readout (PC1 and PC3) located at radii of 2, 2.5, and 5 m, respectively [26]. For each analysis, the collision vertex z

along the beam direction was constrained to be within $|z| < 30$ cm. A confirmation hit within a 2σ matching window was required in PC3 to eliminate most albedo, conversions, and decays. Particle momenta were measured with resolutions $\delta p/p = 0.7\% \oplus 0.91\% p$, $\delta p/p = 0.6\% \oplus 3.6\% p$, and $\delta p/p = 0.7\% \oplus 1.0\% p(\mathrm{GeV}/c)$ at $\sqrt{s_{NN}} = 62.4$, 130, and 200 GeV, respectively.

Event centralities were obtained at $\sqrt{s_{NN}} = 62.4$ GeV via a series of cuts on the analog response of the PHENIX beam counters (BBC). For $\sqrt{s_{NN}} = 130$ and 200 GeV, cuts in the space of BBC versus zero-degree calorimeter analog response were employed; they reflect percentile cuts on the total interaction cross section at each beam energy [27]. Estimates for the number of participant nucleons N_{part} were also made for each of these cuts following the Glauber-based model detailed in Ref. [27]. Systematic uncertainties associated with these determinations are estimated to be less than $\sim 10\%$ for central and midcentral collisions.

The differential v_2 measurements reported in this Letter have been obtained via three separate methods of analysis:

First, we used the reaction plane technique which correlates the azimuthal angles of charged tracks detected in the central arms with the azimuth of an estimated event plane Φ_2, determined via hits in the north and south BBC's located at $|\eta| \sim 3$–3.9 [18]. This method was used for the analysis of data taken at both $\sqrt{s_{NN}} = 62.4$ and 200 GeV. Corrections [18,28] were applied to account for possible azimuthal distortions in the distribution of the estimated reaction planes. Values of v_2 were calculated via the expression

$$v_2 = \frac{\langle \cos(2(\phi - \Phi_2)) \rangle}{\langle \cos(2(\Phi_2 - \Phi_{RP})) \rangle}, \quad (1)$$

where the denominator represents a resolution factor which corrects for the difference between the estimated and the true azimuth of the reaction plane Φ_{RP} [18,28]. The estimated resolution of the combined reaction plane from both BBC's [18] has an average of 0.33(0.16) over centrality with a maximum of about 0.42(0.19) for $\sqrt{s_{NN}} =$ 200(62.4) GeV. Thus, the estimated correction factor, which is the inverse of the resolution for the combined reaction plane, ranges from 2.4(5.4) to 5.0(13).

Second, we performed a cumulant analysis on data collected at $\sqrt{s_{NN}} = 200$ and 62.4 GeV to obtain the anisotropy directly [29]

$$\langle e^{2i(\phi_1 - \phi_2)} \rangle = \langle e^{2i\phi_1} \rangle \langle e^{-i2\phi_2} \rangle + \langle\langle e^{2i(\phi_1 - \phi_2)} \rangle\rangle, \quad (2)$$

where the double brackets denote an average over pairs of particles emitted in an event followed by further averaging over events. For a detector having full azimuthal acceptance, the averages $\langle e^{2i\phi_1} \rangle$ and $\langle e^{-2i\phi_2} \rangle$ vanish due to symmetry considerations to give the second order cumulant estimate $v_2\{2\}$ [29] of v_2

$$\langle\langle e^{2i(\phi_1 - \phi_2)} \rangle\rangle = v_2\{2\}^2. \quad (3)$$

Since PHENIX does not have full azimuthal acceptance, $\langle e^{2i\phi_1} \rangle$ and $\langle e^{-2i\phi_2} \rangle$ do not vanish and this leads to an initial underestimate of the extracted anisotropy. To correct for this underestimate, separate correction factors ($\sim 30\%$) were evaluated and applied for each centrality and p_T cut, at each collision energy, following the procedures detailed in Ref. [29].

Third, we extracted the anisotropy at $\sqrt{s_{NN}} = 62.4$, 130, and 200 GeV via assorted two-particle correlation functions [11,18]: $C(\Delta\phi) = N_{\mathrm{cor}}(\Delta\phi)/N_{\mathrm{mix}}(\Delta\phi)$, where $N_{\mathrm{cor}}(\Delta\phi)$ is the observed $\Delta\phi$ distribution for charged particle pairs selected from the same event, and $N_{\mathrm{mix}}(\Delta\phi)$ is the $\Delta\phi$ distribution for particle pairs selected from mixed events. Mixed events were obtained by randomly selecting each member of a particle pair from different events with the same multiplicity and vertex cuts.

To extract the anisotropy of these correlations, two correlation functions were generated for each p_T and centrality selection [11,18]. For the first, charged hadron pairs were formed by selecting both particles from a reference range $p_{T,\mathrm{ref}}$, which excluded the p_T range of interest (i.e., a reference correlation). For the second, assorted hadron pairs were formed by selecting one member from the p_T range of interest and the other from $p_{T,\mathrm{ref}}$. The elliptic flow v_2 was obtained via the ratio $A_{2,a}/\sqrt{A_{2,\mathrm{ref}}} = v_2$, where $A_{2,a}$ and $A_{2,\mathrm{ref}}$ are the anisotropies extracted from the assorted and reference correlation functions (respectively) with the fit function:

$$C(\Delta\phi) = a_1[1 + 2A_2 \cos(2\Delta\phi) + \lambda e^{[-0.5(\Delta\phi/\sigma)^2]}], \quad (4)$$

where the Gaussian and harmonic terms are used to characterize the asymmetry (at small $\Delta\phi$) and the anisotropy of the correlation function, respectively [11,13].

Figure 1 shows representative $\Delta\phi$ correlation functions obtained for charged hadrons detected in the PHENIX central arms ($-0.35 < \eta < 0.35$) at $\sqrt{s_{NN}} = 62.4$ GeV. Correlation functions for midcentral events (centrality = 20%–40%) are shown for hadrons with $0.5 < p_T < 0.7$ GeV/c and $1.0 < p_T < 1.5$ GeV/c in Fig. 1(a) and Fig. 1(c), respectively. The same p_T cuts have been made for the correlation functions shown in Figs. 1(b) and 1(d) but for more peripheral collisions (centrality = 40%–60%). For both sets of correlation functions $0.65 < p_{T,\mathrm{ref}} < 2.5$ GeV/c. Figures 1(a)–1(d) show a clear anisotropic pattern with relatively small asymmetries (0°/180° ratios). Such asymmetries have been attributed to small jet contributions to the correlation functions [11,13], and are expected to decrease with decreasing $\sqrt{s_{NN}}$. The curves in Fig. 1 indicate a fit to the correlation function with Eq. (4); they show an increase of the anisotropy with increasing impact parameter and p_T. These trends are similar to those of prior AGS, SPS, and RHIC measurements [16,23,24,30] and are consistent with the expected patterns for in-plane elliptic flow [5,7].

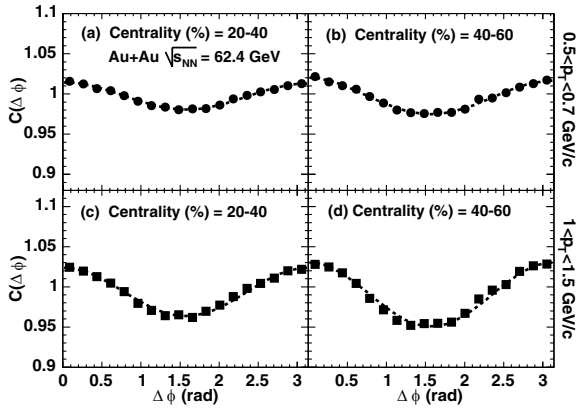

FIG. 1. Assorted-p_T correlation functions ($0.65 < p_{T,\mathrm{ref}} < 2.5$ GeV/c) for charged hadrons of $0.5 < p_T < 0.7$ GeV/c (top panels) and $1.0 < p_T < 1.5$ GeV/c (bottom panels) obtained in Au + Au collisions at $\sqrt{s_{NN}} = 62.4$ GeV. The left and right panels show correlation functions for centrality cuts of 20%–40% and 40%–60%, respectively. The lines represent fits to the correlation functions (see text).

Figure 2 compares the differential anisotropy $v_2(p_T)$, obtained at $\sqrt{s_{NN}} = 62.4$ GeV for all three methods of extraction. The error bars shown indicate statistical errors. Systematic errors are estimated to be ~10%, 5%, and 5% for extractions via the reaction plane, cumulant, and correlation function methods of analysis, respectively. The results, which are shown for two separate centrality cuts (0%–20% and 20%–40%) in each case, indicate an initial increase of v_2 with p_T followed by the previously observed plateau for $p_T \gtrsim 2.5$ GeV/c [11,17]. The close agreement of $v_2(p_T)$ values obtained from the cumulant and correlation function methods of analysis serve to confirm the reliability of these methods of extraction. On the other hand, the agreement between results from these latter methods and that obtained from the reaction plane method is quite striking, given the large rapidity gap (~3 units) between the particles used for reaction plane determination and the midrapidity particles correlated with this plane. It is expected that the latter correlations are less influenced by nonflow contributions, especially for $p_T < 2.0$ GeV/c. Consequently, we attribute this agreement to the absence of strong nonflow contributions to the hadron correlations (for $p_T < 2.0$ GeV/c) at midrapidity. A similarly good agreement between the different methods of analysis was obtained for all centralities presented in this work.

Figure 3 compares the centrality and p_T dependence (respectively) of the anisotropy obtained at several collision energies. The circles, stars, and squares in Fig. 3(a) show $v_2(N_{\mathrm{part}})$ for $\langle p_T \rangle$ selections of 0.4, 0.75, and 1.35 GeV/c obtained via the cumulant and correlation function methods of analysis. The same results obtained via the reaction plane method are consistent with prior results [18]. The open and filled symbols show measurements performed at $\sqrt{s_{NN}} = 62.4$ and 130 (200) GeV as indicated; they show rather striking agreement between the magnitudes of the v_2 values obtained at all three collision energies. Further evidence that this agreement persists down to $\sqrt{s_{NN}} = 62.4$ GeV is given in Fig. 3(b). The open and filled circles compare the differential anisotropy $v_2(p_T)$, obtained at $\sqrt{s_{NN}} = 62.4$ and 200 GeV for the 13%–26% most central collisions ($\langle N_{\mathrm{part}} \rangle = 200$). The comparison indicates that $v_2(p_T)$ saturates above 2 GeV/c independent of beam energy. Such a saturation is compatible with surface emission from a relatively opaque source [22]. More importantly, very little change in v_2 is observed as the collision energy is raised from $\sqrt{s_{NN}} = 62.4$ to 200 GeV. The latter contrasts with the much lower v_2 values measured in Pb + Pb collisions (filled squares) by the CERES Collaboration at $\sqrt{s_{NN}} = 17.2$ GeV for the same centrality cut (13%–26%) [23].

Figure 4 summarizes the $\sqrt{s_{NN}}$ dependence of v_2 for charged hadrons produced in Au + Au collisions for two separate p_T selections (0.65 and 1.75 GeV/c) and

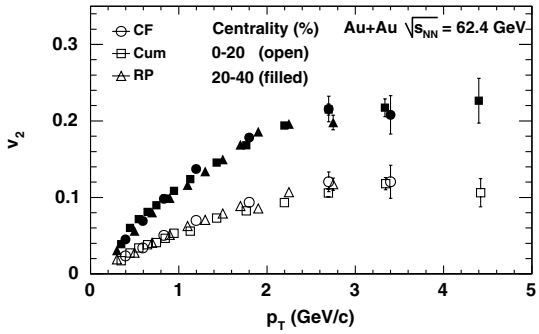

FIG. 2. Differential anisotropy $v_2(p_T)$ for charged hadrons in Au + Au collisions at $\sqrt{s_{NN}} = 62.4$ GeV with centrality cuts of 0%–20% (open symbols) and 20%–40% (filled symbols), obtained via the methods of correlation functions (CF), cumulants (Cum), and reaction plane (RP).

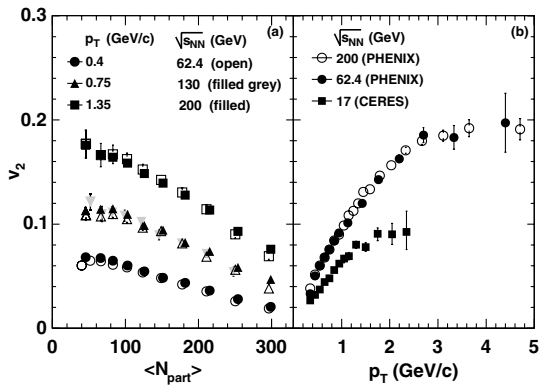

FIG. 3. Differential anisotropy $v_2(N_{\mathrm{part}})$ (left) and $v_2(p_T)$ (right) for several energies as indicated. $v_2(p_T)$ is shown for the centrality selection 13%–26% ($\langle N_{\mathrm{part}} \rangle = 200$) which facilitates a comparison with CERES data (filled squares) from Ref. [23].

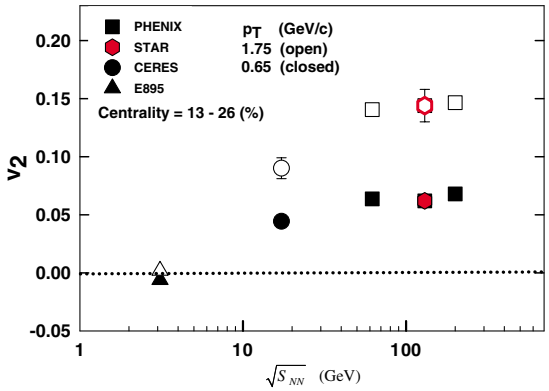

FIG. 4 (color online). Differential v_2 vs $\sqrt{s_{NN}}$ for charged hadrons in nucleus-nucleus collisions. Results are shown for the centrality cut of 13%–26% and p_T selections of 1.75 GeV/c (open symbols) and 0.65 GeV/c (closed symbols). The STAR, CERES, and E895 data are taken from Refs. [17,23,30–32], respectively.

centrality = 13%–26%. These data are taken from the current measurements and earlier measurements at the SPS [23] and the AGS [30–32]. The AGS [E895] measurements [30–32] are for protons but the transition energy is not very different for pions and protons. The STAR results were obtained for a slightly different centrality selection (10%–30%) [17] having essentially the same mean centrality. For both p_T cuts, the magnitude of v_2 shows a significant increase with collision energy (~50% increase from SPS to RHIC) up to the energy $\sqrt{s_{NN}} = 62.4$ GeV. Thereafter, it appears to saturate for larger beam energies. We note that this saturation is not in conflict with the recent observation of an increase of the p_T-integrated v_2 with $\sqrt{s_{NN}}$ [25]. The latter increase is expected if the $\langle p_T \rangle$ increases with $\sqrt{s_{NN}}$.

To summarize, we have measured differential azimuthal anisotropies for charged hadrons in Au + Au collisions spanning the energy range $\sqrt{s_{NN}} = 62.4$–200 GeV. Detailed comparisons of these differential measurements indicate no significant collision energy dependence of the anisotropy over this range. By contrast, comparisons to differential measurements obtained at AGS and SPS energies indicate that v_2 increases with collision energy up to $\sqrt{s_{NN}} = 62.4$ GeV. The energy density is estimated to increase by approximately 30% over the range $\sqrt{s_{NN}} = 62.4$–200 GeV. In a hydrodynamic scenario v_2 is driven by a pressure gradient which is related to the energy density via the equation of state [5,7]. Thus, the apparent saturation of v_2 above $\sqrt{s_{NN}} = 62.4$ GeV may be indicative of the role of a rather soft equation of state. Such a softening could result from the production of a mixed phase [31] for the range $\sqrt{s_{NN}} = 62.4$–200 GeV. Additional combined measurements of v_2, particle spectra, and the space-time extent of emission sources are required to further constrain the EOS.

We thank the staff of the Collider-Accelerator and Physics Departments at BNL for their vital contributions. We acknowledge support from the Department of Energy and NSF (USA), MEXT and JSPS (Japan), CNPq and FAPESP (Brazil), NSFC (China), IN2P3/CNRS, and CEA (France), BMBF, DAAD, and AvH (Germany), OTKA (Hungary), DAE and DST (India), ISF (Israel), KRF, CHEP, and KOSEF (Korea), RMIST, RAS, and RMAE (Russia), VR and KAW (Sweden), US CRDF for the FSU, US-Hungarian NSF-OTKA-MTA, and US-Israel BSF.

*Deceased.
†PHENIX Spokesperson.
Email: zajc@nevis.columbia.edu

[1] See, for example, the *Proceedings of the Quark Matter Conference, Oakland, CA, 2004* [J. Phys. G 30, S633–S1430 (2004).
[2] J. L. Nagle, nucl-ex/0405012.
[3] M. Gyulassy *et al.*, Nucl. Phys. **A750**, 30 (2005).
[4] B. Muller, nucl-th/0404015.
[5] E. V. Shuryak, Nucl. Phys. **A750**, 64 (2005).
[6] J.-Y. Ollitrault, Phys. Rev. D **46**, 229 (1992).
[7] P. F. Kolb *et al.*, Nucl. Phys. **A696**, 197 (2001).
[8] T. Hirano *et al.*, Nucl. Phys. **A743**, 305 (2004).
[9] M. Gyulassy, I. Vitev, and X. N. Wang, Phys. Rev. Lett. **86**, 2537 (2001).
[10] Y. Kovchegov *et al.*, Nucl. Phys. **A708**, 413 (2002).
[11] N. N. Ajitanand *et al.*, Nucl. Phys. **A715**, 765 (2003).
[12] M. Chiu *et al.*, Nucl. Phys. **A715**, 761 (2003).
[13] C. Adler *et al.*, Phys. Rev. Lett. **90**, 082302 (2003).
[14] S. S. Adler *et al.*, nucl-ex/0408007.
[15] J. Rak, J. Phys. G **30**, S1309 (2004).
[16] K. Adcox *et al.*, Phys. Rev. Lett. **89**, 212301 (2002).
[17] C. Adler *et al.*, Phys. Rev. C **66**, 034904 (2002).
[18] S. S. Adler *et al.*, Phys. Rev. Lett. **91**, 182301 (2003).
[19] M. Bleicher *et al.*, Phys. Lett. B **526**, 309 (2002).
[20] R. J. Fries, B. Muller, C. Nonaka, and S. A. Bass, Phys. Rev. C **68**, 044902 (2003).
[21] J. Adams *et al.*, Phys. Rev. Lett. **92**, 052302 (2004).
[22] D. Molnar, nucl-th/0503051.
[23] G. Agakichiev *et al.*, Phys. Rev. Lett. **92**, 032301 (2004).
[24] C. Alt *et al.*, Phys. Rev. C **68**, 034903 (2003).
[25] B. Back *et al.*, Phys. Rev. Lett. **94**, 122303 (2005).
[26] K. Adcox *et al.*, Nucl. Instrum. Methods Phys. Res., Sect. A **499**, 469 (2003).
[27] K. Adcox *et al.*, Phys. Rev. C **69**, 024904 (2004).
[28] A. M. Poskanzer and S. A. Voloshin, Phys. Rev. C **58**, 1671 (1998).
[29] N. Borghini, P. M. Dinh, and J. Y. Ollitrault, Phys. Rev. C **64**, 054901 (2001).
[30] P. Chung *et al.*, Phys. Rev. C **66**, 021901 (2002).
[31] P. Danielewicz *et al.*, Science **298**, 1592 (2002).
[32] C. Pinkenburg *et al.*, Phys. Rev. Lett. **83**, 1295 (1999).